DOI: 10.1002/anie.201201084

Graphene Synthesis

From Nanographene and Graphene Nanoribbons to Graphene Sheets: Chemical Synthesis

Long Chen, Yenny Hernandez, Xinliang Feng, and Klaus Müllen**

carbon · graphene · nanostructures · surface synthesis · synthesis design

Graphene, an individual two-dimensional, atomically thick sheet of graphite composed of a hexagonal network of sp^2 carbon atoms, has been intensively investigated since its first isolation in 2004, which was based on repeated peeling of highly oriented pyrolyzed graphite (HOPG). The extraordinary electronic, thermal, and mechanical properties of graphene make it a promising candidate for practical applications in electronics, sensing, catalysis, energy storage, conversion, etc. Both the theoretical and experimental studies proved that the properties of graphene are mainly dependent on their geometric structures. Precise control over graphene synthesis is therefore crucial for probing their fundamental physical properties and introduction in promising applications. In this Minireview, we highlight the recent progress that has led to the successful chemical synthesis of graphene with a range of different sizes and chemical compositions based on both top-down and bottom-up strategies.

1. Introduction

Fullerenes and carbon nanotubes (CNTs) are synthetic carbon allotropes that have sphere (quasi-0-dimensional) and hollow cylindrical (quasi-1-dimensional) structures, respectively. Since their discovery in 1985[1] and 1991,[2] these two carbon materials have received tremendous attention because of their remarkable physical properties and novel chemical behavior. Fullerenes are mainly produced through the vaporization of graphite by resistive heating under carefully defined conditions or the combustion of hydrocarbons in fuel-rich flames. CNTs can be prepared in sizeable quantities by means of arc discharge, laser ablation, and chemical vapor deposition (CVD). In contrast, there also exists a total organic synthesis strategy towards fullerenes and CNTs from defined aromatic precursor molecules.[3] Graphene, an individual two-dimensional, atomically thick sheet of graphite composed of a hexagonal network of sp^2-hybridized carbon atoms, can be considered as the 'mother' of fullerenes (wrapped graphene), carbon nanotubes (rolled graphene), and other graphitic forms. It has been intensively investigated since its isolation in 2004, when Geim, Novoselov et al. reported a micromechanical cleavage approach for the exfoliation of graphite based on repeated peeling of highly oriented pyrolyzed graphite (HOPG).[4] The pioneering experiments of the Manchester team to characterize the physical properties of graphene were recognized with the 2010 Nobel Prize in physics.[5] The extraordinary electronic, thermal, and mechanical properties of graphene make it a promising candidate for practical applications in electronics,[6] sensing,[7] catalysis,[8] energy storage[9] and conversion,[10] as well as biological labeling.[11] Nevertheless, a few challenges remain for the implementation of graphene in electronics.[12] For instance, as it was stressed at the meeting of "Graphene: The Road to Applications" which was held in Cambridge, Massachusetts, on 11–13 May, 2011, the greatest obstacle at present is the lack of an efficient way to reliably produce graphene in both large quantities and high quality.[13] Another difficulty lies in the lack of a controllable synthesis of graphene with defined size, shape, and edge structure, which is crucial to opening up the energy band gap of graphene and allow its introduction as an active material in field-effect transistors (FETs).[14]

Two distinct strategies have been established for graphene synthesis: exfoliating graphite towards graphene (top-down) and building up graphene from molecular building blocks

[*] Dr. L. Chen, Dr. Y. Hernandez, Prof. X. Feng, Prof. K. Müllen
Max Planck Institute for Polymer Research
Ackermannweg 10, 55122 Mainz (Germany)
E-mail: feng@mpip-mainz.mpg.de
muellen@mpip-mainz.mpg.de
Prof. X. Feng
College of Chemistry and Chemical Engineering
Shanghai Jiao Tong University, 800 Dongchuan Road
Shanghai, 200240 (People's Republic of China)

(bottom-up).[15] The top-down methods typically include mechanical exfoliation of HOPG,[4] solution-based exfoliation of graphite intercalation compounds (GICs),[16] and chemical oxidation/exfoliation of graphite followed by reduction of graphene oxide (GO).[17] The bottom-up approaches for graphene synthesis comprise epitaxial growth on metallic substrates by means of CVD,[18] thermal decomposition of SiC,[19] and organic synthesis[20] based on precursor molecules.[21]

While there have been several excellent reviews on the synthesis of graphene and their applications in electronics, composites, and energy storage/conversion, these articles are mainly focused on graphene oxide or on chemically derived graphene.[22] We noted however that a more general overview on graphene synthesis according to its chemical nature is missing. In contrast, there have been a significant number of publications addressing the synthesis and application of graphene nanoribbons, nanographenes, and graphene dots, where the size/dimension definition for these graphene nanostructures remains very vague.[22c] All these issues prompted us to organize this review as a summary of the recent progress on the chemical synthesis of graphene spanning different sizes, thereby placing special emphasis on solution and surface synthesis approaches.

Cutting graphene sheets into narrow strips yields graphene nanoribbons (GNRs). For many decades, GNRs have been of interest because of their theoretically predicted physical properties.[23] GNRs can be thought of as planar analogues of CNTs, with band gaps depending upon the ribbon width. Thus, producing GNRs with defined widths and edge structures constitutes a great challenge that many chemists and materials scientists have sought to tackle. GNRs display a finite band gap when their width is less than 10 nm. In the context of this review, GNRs will be defined as a graphene strip with a width of less than 10 nm and with a large aspect ratio (generally, the length/width should be higher than 10; Figure 1).[16a,20b,21a] Nevertheless, we also note that there are a few papers reporting the fabrication of GNRs of widths of up to 50 nm while maintaining a large aspect ratio.[53,58] To avoid such confusion, we classify those graphene nanostructures as quasi-GNRs.

Polycyclic aromatic hydrocarbon (PAH), is a common name given to aromatic hydrocarbons which contain more than two unsubstituted fused benzene rings. Based on the chemical nomenclature of 35 fused PAHs recognized by the

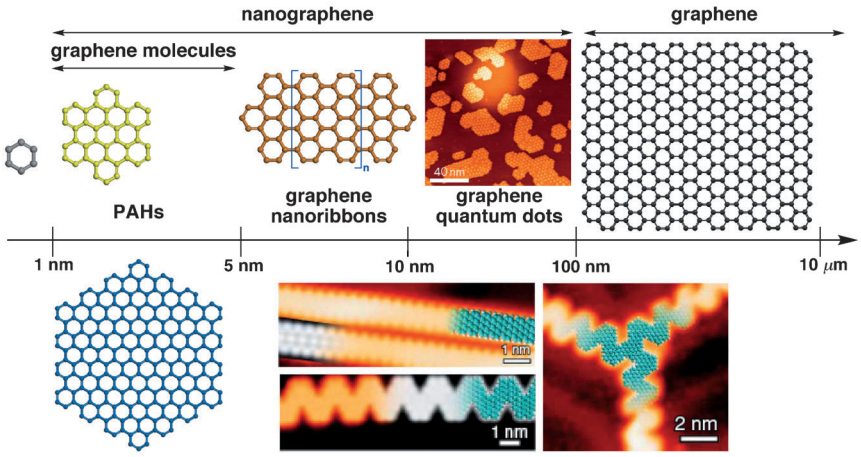

Figure 1. Schematic illustration of graphene terminology defined according to their size scale. Graphene molecules are a subset of graphene with size between 1–5 nm; GNRs are defined as graphene strips with a width <10 nm while maintaining a length/width ratio of >10. GQDs are relatively regularly shaped graphene units with sizes ranging from several to 100 nm. Nanographene units are graphene fragments with diameters of <100 nm, while graphene should exceed 100 nm in both directions. The STM images of GQDs modified with permission from Ref. [67]; two STM images of GNRs modified with permission from Ref. [21a]; copyright 2010, Nature publishing group.

Xinliang Feng obtained his PhD in 2008 under the supervision of Prof. K. Müllen at the Max Planck Institute (MPIP) for Polymer Research. In December 2007, he was appointed a project leader at MPIP. He became a professor at Shanghai Jiao Tong University in 2010 and was appointed director of the Institute of Advanced Organic Materials. His current scientific interests include the graphene, organic conjugated materials, carbon-rich molecules, and materials for electronic and energy-related applications.

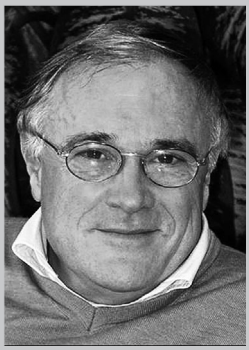

Klaus Müllen received his PhD in 1972 at the University of Basel. He pursued postdoctoral research with Prof. J. F. M. Oth at ETH Zurich, where he obtained his habilitation in 1977. He was a Professor of Organic Chemistry at the Universities of Cologne and Mainz, and became a member of the Max Planck Society in 1989 where he was appointed Director of the Department for Synthetic Chemistry at the Max Planck Institute for Polymer Research. His current research focuses on synthetic macromolecular chemistry, supramolecular chemistry, and materials science.

1957 IUPAC rules,[24] it is reasonable to define the term graphene molecule[25] as large PAHs having sizes of 1–5 nm, while nanographene can be a graphene fragment ranging from 1 to 100 nm in size. Once the size of the hexagonal sp^2 carbon network exceeds 100 nm, they can be directly regarded as graphene.[25]

How can scientists ever get access to precise graphene nanostructures to probe their fundamental physical properties for their introduction in promising applications? This review describes work from our laboratory and others, work that has led to the successful chemical synthesis of graphene of different sizes and chemical compositions by using both top-down and bottom-up strategies.

2. Synthesis of Graphene

2.1. Liquid-Phase Exfoliation of Graphene

Undoubtedly, graphite is the most important source for obtaining isolated graphene sheets. Natural graphite has been exfoliated in a range of organic solvents such as *N*-methylpyrrolidone (NMP)[26] and *N*,*N*-dimethylformamide (DMF).[27] Exfoliation occurs because of the strong interaction between the solvent and the graphitic basal planes, that is, the energetic penalty for exfoliation and subsequent dispersion is minimized. Solvents with surface tensions of about $40\,mJ\,m^{-2}$ are generally good candidates for exfoliation. Transmission electron microscopy (TEM) and electron diffraction (ED) measurements reveal the presence of a large number of monolayer graphene sheets of high crystal quality. The monolayer production yield was calculated to be approximately 1 wt% based on the statistic analysis. The production of defect-free graphene sheets in the liquid phase may allow chemists and material scientists to have large-scale access to defect-free graphene for further processing.

Graphene can also be produced in the liquid phase by sonicating tetrabutylammonium hydroxide (TBA) and oleum-intercalated graphite in DMF to obtain high quality graphene sheets, which can be fabricated into transparent conducting films by Langmuir-Blodgett deposition.[28] The weakened van der Waals interaction in intercalated graphite compounds allows for easier dispersion in organic solvents, as it has been recently demonstrated by the successful liquid-phase exfoliation.[29] Transparent electrodes prepared from solution-exfoliated graphene have been reported. However, the large interjunction resistance of the prepared films caused by the residual surfactants limits their application when compared to indium-tin oxide (ITO).[30] These solution-processed transparent graphene electrodes have been utilized in liquid crystal devices[27] and flexible electrodes.

As in the case of CNTs, natural graphite has also been reported to be exfoliated in aqueous surfactant solutions, and is convenient for further solution processing. Sodium dodecyl benzene sulfonate (SDBS) and sodium cholate (SC) can serve as good candidates for exfoliation when used at concentrations below their critical micelle concentrations (CMCs).[31] The dispersed graphene sheets become electrostatically charged, as confirmed by zeta potential measurements, thus making these dispersions more sensitive to pH changes. In particular, sodium cholate allows exfoliation of graphene in high yields, thus reaching a concentration of up to $0.04\,mg\,mL^{-1}$. As with organic solvent exfoliation, the graphene layers exfoliated in aqueous dispersions are also defect free. The good processability of this approach allows the deposition on insulating substrates and the preparation of transparent electrodes by vacuum filtration. Nevertheless, graphene is polydispersed in the liquid phase and its isolation is somewhat challenging. In a recent report, graphene multilayers in solution, which have different buoyant densities, can be separated by the density gradient ultracentrifugation (DGU) to yield fractions of graphene.[32] This technique has been scaled up to produce commercially available graphene in aqueous solutions.

Graphene has also been dispersed in the presence of of 1-pyrenecarboxylic acid[33] to produce aqueous dispersions in relatively high yields. Additionally, graphene has been prepared by supercritical fluidic exfoliation in organic solvents and in ethanol solutions containing the sodium salt of 1-pyrenesulfonic acid.[34] Furthermore, soluble expanded graphite derived from fluorine intercalated graphite compounds have been exfoliated in SDBS solutions or organic solvents to attain stable dispersions of large graphene sheets which were subsequently used for transparent electrode applications.[35]

All of the methods discussed so far use ultrasonic energy to drive the exfoliation, and generally diminishes the size of the produced graphene flakes, especially when long sonication processes are required. Spontaneous graphite exfoliation towards graphene in charged liquid media is therefore appealing. The first report in this direction was achieved by the spontaneous dissolution of potassium intercalated graphite compounds in NMP to produce graphene dispersions.[36] Later, reduced graphene sheets were obtained from spontaneously dissolved graphite intercalation compounds which had been synthesized in dispersions of liquid sodium/potassium alloys using 1,2-dimethoxyethane (DME) as an inert and electride/alkalide stabilizing solvent. On the basis of this result, the first wet chemical graphene functionalization was demonstrated by the reaction of aryl diazonium compounds with in situ activated, exfoliated, and reduced graphene.[37] Several other approaches have been reported, such as exfoliation driven by negatively charged complexes in polycarbonate electrolytes,[38] electrochemical exfoliation of HOPG crystals in sulfuric acid to produce single and multilayer graphene, which can be subsequently dispersed in DMF to obtain high concentrations of dispersions,[39] as well as the spontaneous graphite exfoliation in chlorosulfonic acid which achieves a concentration of approximately $2\,mg\,mL^{-1}$.[40] Additionally, few-layer graphene can be obtained from ball milling of graphite with melamine under a nitrogen atmosphere and subsequent dispersion of the milled material in water or DMF at relatively high concentrations (ca. $0.2\,mg\,mL^{-1}$).[41]

Apart from the solution exfoliation of high quality graphene from graphite, graphene oxide (GO), as a result of its easy availability and solution processability, represents thus far the most popular source of graphene derivatives for chemists and material scientists. GO can be prepared using

the modified Staudenmaier and Hummers method involving a strong acid and oxidant for which the oxidation level is strongly governed by the reaction conditions and the graphite precursors used.[42] The structural defects generated during chemical reaction disrupt the electronic structure of graphene, thus giving rise to a sheet resistance several orders of magnitude higher for GO compred to that of pristine graphene. Chemical or thermal reduction of GO is required to recover the electrical properties. However, the complete reduction of GO to perfect graphene has not been achieved so far.[43] As there have been several outstanding reviews on the chemistry of GO and its composites, further discussion here is unwarranted; rather, we recommend the reader to refer to the recent reviews.[42]

2.2. Graphene Growth by Using the CVD Method

The CVD method has been used extensively for the growth of carbon nanotubes in high yields in the presence of catalytic amounts of nanoparticles.[44] The chemical nature of the metal catalysts and carbon sources plays a key role in the growth of carbon nanotubes. This technique has also proven efficient for producing large-area graphene layers on transition-metal surfaces[45] such as platinum,[46] ruthenium,[18b,47] nickel,[48] and copper.[49] CVD-grown graphene, on copper,[50] can be produced in large areas with very few structural defects.[51] Remarkable progress on CVD graphene synthesis has been achieved in the last two years. Bae et al. reported growing a monolayer graphene 30 inches in size on copper.[51] Further, a roll-to-roll technique similar to a newspaper printing process, has been used to transfer graphene onto various substrates (Figure 2a). After chemical doping with HNO_3, the performance of a transparent electrode made of CVD graphene exceeded that of ITO with a sheet resistance as low as approximately 30 Ω per square unit at about 90% of light transmission. This technological milestone indicates that graphene can be a viable alternative for ITO and may dramatically reduce the cost of transparent conductors.

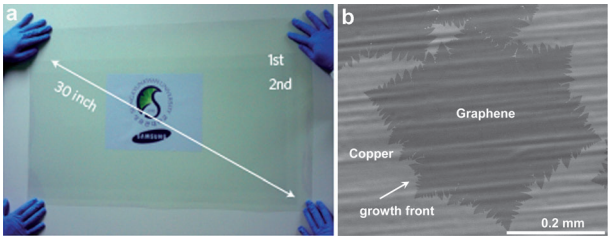

Figure 2. a) A transparent ultralarge-area graphene film transferred on a 35 inch polyethylene terephthalate (PET) sheet. Reproduced with permission from Ref. [51]. Copyright 2010, Nature publishing group. b) SEM images of graphene domain grown at 1035 °C on copper by CVD. Scale bar: 0.2 mm. Reproduced with permission from Ref. [52]. Copyright 2011, American Chemical Society.

Nevertheless, the presence of domain boundaries in CVD graphene has been found to be detrimental to its transport properties. To achieve the quality comparable to a mechanically exfoliated graphene, growing large-area graphene single crystals will be highly desirable. By applying low-pressure CVD in copper foil enclosures with methane as a carbon precursor, it was possible to obtain graphene single crystals with sizes of up to 0.5 mm (Figure 2b). Based on such graphene films, the electron mobility extracted from FET measurements was found to be higher than $4000\ cm^2\,V^{-1}\,s^{-1}$.[52] While the CVD growth of graphene on nickel surface occurs through the carbon segregation, in the case of copper the growth is driven through a surface adsorption process.[53] The significant difference of the solubility of carbon in melting nickel and copper is what determines the number of layers and the quality of the graphene grown on these two metals. Since only a small amount of carbon can be dissolved in copper, growth terminates once the surface is fully covered with graphene. In contrast, nickel can dissolve more carbon atoms on its surface and hence it is difficult to get uniform graphene films because of precipitation of the extra carbon during the cooling process.

CVD is mostly limited to the use of gaseous carbon sources, thus making it difficult to apply the technology to a wider variety of potential feedstocks. In a recent report, a large-area and high quality graphene film from solid carbon sources atop a metal substrate was realized.[54] In this case, a poly(methyl methacrylate) (PMMA) thin film was spin coated onto a copper film, which was additionally subjected to heat treatment at a temperature as low as 800 °C under a reductive gas flow. Nitrogen-doped graphene could be also synthesized through this one-step process.[54] In general, the replacement of metal surfaces for graphene growth remains a big challenge. Very recently, a metal-catalyst-free synthesis of high quality polycrystalline graphene on a dielectric substrate (SiO_2) was developed.[55] Oxygen-aided activation of the substrate was a crucial step. The growth mechanism is analogous to that of single-wall carbon nanotube growth on SiO_2. Therefore, this work demonstrated the avoidance of using either a metal catalyst or a complicated transfer process, thus facilitating the device fabrication.

Several groups have reported the patterning of copper islands on insulating substrates to grow defined-area graphene, however, this approach has not proven efficient because of the migration of the copper atoms on the substrates when subjected to high temperature treatment.[56] Careful preparation of copper substrates allows the growth of the graphene domains of defined shape and edge structure. However, this process must be scaled up to fully assess the advantage that an expensive substrate preparation would bring to commercial applications.

2.3. Synthesis of Graphene Nanoribbons

Although the opening of the band gap in bilayer graphene through an electric field has been studied, such an approach is not efficient because of the difficulty in accessing double-layer graphene with AB stacking.[57] Therefore, cutting the graphene into small strips, namely GNRs, seems to be the most straightforward manner to reproducibly fabricate gra-

phene with tailorable band gaps. Generally, two approaches have been explored for the top-down synthesis of GNRs. The first is the cutting or etching of graphene or graphite precursors into narrow graphene strips; the second is the longitudinal unzipping of carbon nanotubes to corresponding GNRs.

2.3.1. Graphene Cutting for the Production of GNRs

In 2007, e-beam patterning and oxygen (O_2) plasma etching on mechanically exfoliated graphene was reported to make the first sub-50 nm nanoribbons (or quasi-GNRs).[58] Although the process yielded I_{on}/I_{off} ratios of up to 10^4, the performance of the FETs based on GNRs showed high variability as a result of the lack of control over the edge structure. Further optimization of this approach was developed in 2009 by employing chemically synthesized nanowires as the physical protection mask in oxygen plasma etching (Figure 3), thus allowing the fabrication of GNRs with controllable widths down to 6 nm.[59] The authors also fabricated FETs with nanoribbons directly connected to bulk graphene electrodes. Electrical measurements on an 8 nm wide GNR showed room temperature transistor behavior with an on/off ratio around 160, thus indicating appreciable band gaps arising as a result of lateral quantum confinement effects. It was also found that the $\log(I_{on}/I_{off})$ of devices was inversely proportional to the ribbon width.

The first solution approach for producing quasi-GNRs (with widths down to 10 nm) directly from bulk graphite was reported in 2008 (Figure 4).[16a] First, expanded graphite was prepared by intercalation with sulfuric acid and nitric acid, followed by rapid heating (60 s) to 1000 °C in H_2/Ar, which led to graphite exfoliation into pillars of a few layered graphene sheets. Subsequently, the sonication of this precursor in the presence of poly(*m*-phenylene-vinylene-2,5-dioctoxy-*p*-phenylenevinylene) (PmPV) gave rise to a stable dispersion of GNRs. In this process, sonication served as a mechanical

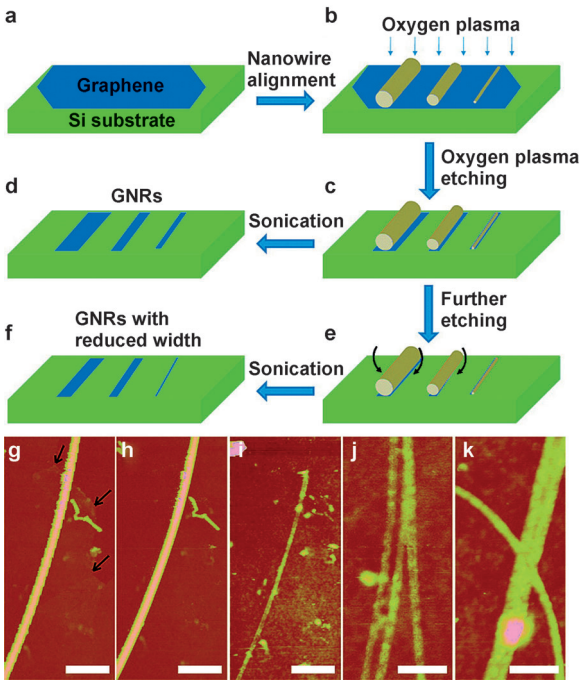

Figure 3. a–f) Schematic fabrication process to obtain GNRs by an oxygen plasma etch with a nanowire etch mask. g, h) AFM images of a nanowire etch mask before (g) and after (h) oxygen plasma etch. i) AFM image of the resulting GNR after sonication removing smaller fragments and the noncovalent interactions between the mask nanowire. j,k) Branched and crossed graphene nanostructures from merged and crossed nanowire masks. Reproduced with permission from Ref. [59]. Copyright 2009, American Chemical Society.

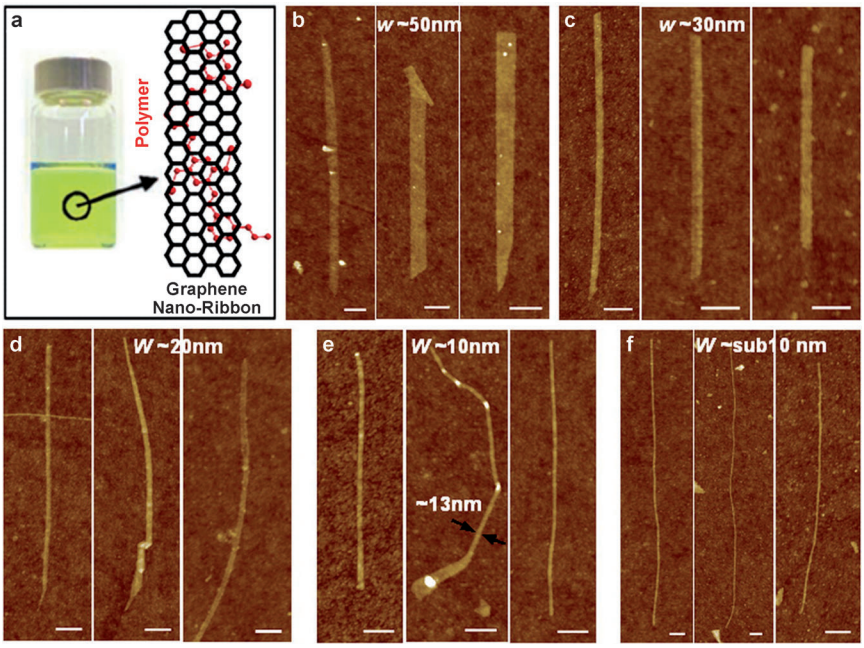

Figure 4. a) Solution of PmPV polymer with suspended GNRs. b–f) AFM images of GNRs with different widths. Scale bar: 100 nm. Reproduced with permission from Ref. [16a]. Copyright 2008, American Association for the Advancement of Science.

driving force to break down graphene sheets into copolymer and graphene fragments to prevent their re-aggregation, thus resulting in the successful isolation of GNRs deposited on a surface. In this work, the band gap (E_g) of GNRs was inversely proportional to their width. Typically, an E_g of approximately 0.4 eV for GNR corresponded to a width of 10 nm, which resulted in an I_{on}/I_{off} ratio of up to 10^6. The hole mobility of these ribbons was estimated to be about 100 to 200 $cm^2 V^{-1} s^{-1}$, thus indicating the high quality of the produced GNRs.

The same group devised a controlled hydrogen plasma reaction at 300 °C to etch graphene nanoribbons selectively at the edges over the basal plane.[60] They could obtain narrow GNRs (sub-5 nm) by etching wider ones derived from unzipped multiwalled carbon nanotubes (see next section). The resulting narrow GNRs exhibited semiconducting characteristics with high on/off ratios (ca. 1000) in FETs (Figure 5).

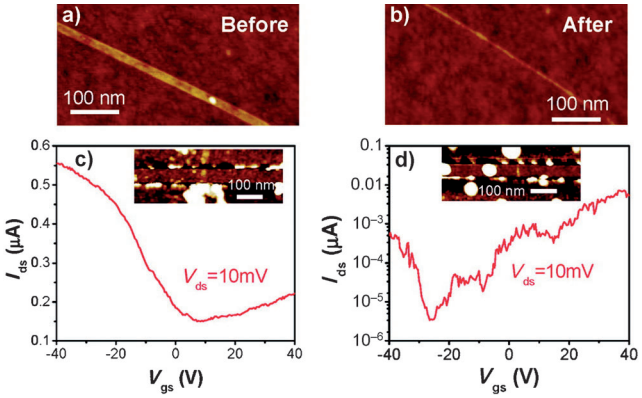

Figure 5. AFM images of a GNR before (a) and after (b) hydrogen plasma edge etching for 55 min. Room-temperature curves of drain-source current (I_{ds}) to gate-source voltage (V_{gs}) of a GNR (width of ≈14 nm) device (c) and a plasma-narrowed GNR (width < 5 nm) device (d). The insets are the AFM images of the corresponding devices. Reproduced with permission from Ref. [60]. Copyright 2010, American Chemical Society.

Recently, a facile way to produce GNR arrays using self-masked plasma etching of CVD-produced graphene with patterned wrinkles was reported.[61] Consistent with the designed wrinkles, the density of the GNR arrays varied from about 0.5 to 5 GNRs μm^{-1}, and more than 88% of the GNRs were less than 10 nm in width. The on/off ratio of such GNR-based FETs was approximately 30, thus indicating an opened band gap. The so-called wrinkle engineering approach enables the production of GNR arrays with band-required widths, which may pave a practical pathway for large-scale integrated GNR devices.

2.3.2. CNT Unzipping for the Production of GNRs

Instead of using graphene or graphite as the precursor, a simple, efficient, and potentially scalable technique for making quasi-GNRs in solution was developed.[62] The starting materials are multiwalled carbon nanotubes (MWCNTs) with diameters between 40 and 80 nm, and this method involves the treatment of nanotubes with concentrated sulfuric acid and potassium permanganate as an oxidizing agent at room temperature with subsequent heating at 55–70 °C (Figure 6). This chemical process enables the unwrapping of CNTs along the longitudinal direction, thus forming ribbons up to 4 μm in length, with widths of 100–500 nm, and thicknesses of 1–30 graphene layers. The mechanism of the unzipping probably involves the oxidation of carbon–carbon double bonds in the nanotubes. The products are highly soluble both in water and polar organic solvents, and is crucial for further processing into electronic devices. Optimization of the reaction conditions by using a second acid (CF_3COOH or H_3PO_4) in the oxidation process was revealed to attain highly crystalline nanoribbons.[63] As proposed in this work, the presence of the second acid (e.g., H_3PO_4) inhibited the creation of vacancies in GNRs because of the protection of the formed diol groups. Interestingly, the degree of oxidation could be adjusted by controlling the amount of the oxidizing agent ($KMnO_4$) in the reaction. Nevertheless, similar to the synthesis of GO, the strong oxidation unavoidably introduces oxygen-containing groups and structural defects into the resulting nanoribbons. Chemical or thermal reduction is required to recover the electrical

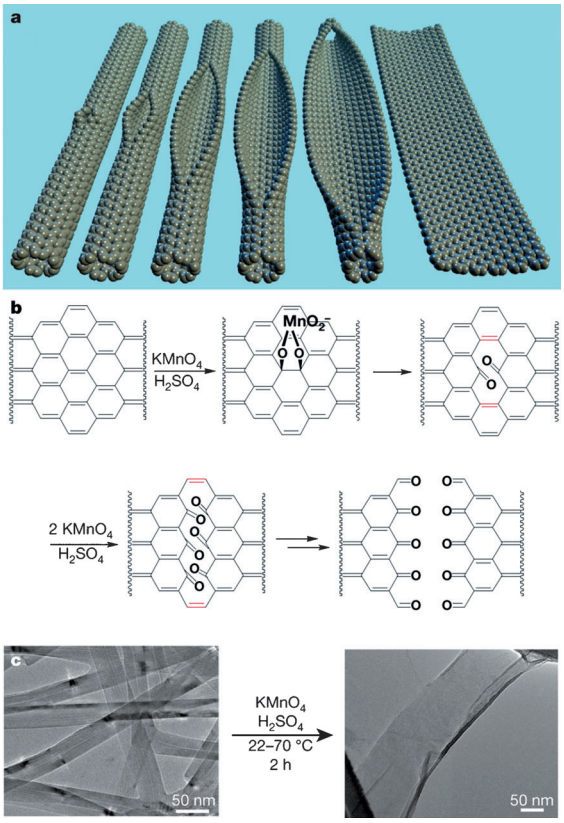

Figure 6. a) Representation of the gradual unzipping of one wall of a carbon nanotube to form a nanoribbon. b) The proposed chemical mechanism of nanotube unzipping. c) TEM images of MWCNTs (left) and the resutl of the transformation into an oxidized graphene nanoribbons (right). Reproduced with permission from Ref. [62]. Copyright 2009, Nature publishing group.

properties of the fabricated GNRs.[62] Another disadvantage of this approach is that the width of the produced ribbons is too wide to open up the band gap as required.

During the course of the above discovery, an alternative approach for unzipping highly crystalline MWCNTs was reported.[64] In this work, dispersed MWCNTs were partly embedded in a poly(methyl methacrylate) (PMMA) layer which served as an etching mask on a silicon substrate (Figure 7). Unzipping was realized by exposing the PMMA-MWCNT film to an Ar plasma treatment. The unmasked area was etched faster than the area shielded by PMMA, thus leading to unzipped GNRs. This strategy renders the fabrication of single-, bi- and multilayer GNRs, depending on the plasma treatment conditions. Finally, the PMMA film was removed by exposing the system to acetone vapor. The ribbons are narrower (10–20 nm wide) than those produced by the solution method.[62] The authors additionally demonstrated the construction of FETs based on these GNRs. For the narrowest ribbons having a width of 6 nm, I_{on}/I_{off} ratios of greater than 100 could be achieved. The charge-carrier mobility of the GNRs is approximately 10 times lower (caused by edge scattering) than that of the two-dimensional graphene sheets.

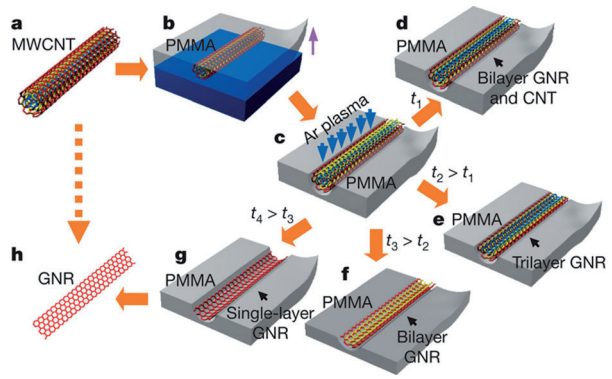

Figure 7. Schematic illustration of making GNRs from CNTs. a) A pristine MWCNT was used as the starting raw material. b) The MWCNT was deposited onto a Si substrate and then coated with a PMMA film. c) The PMMA-MWCNT film was peeled from the Si substrate, turned over, and then exposed to an Ar plasma. d–g) Several possible products were generated after etching for different times: GNRs with CNT cores were obtained after etching for a short time t_1 (d); tri-, bi- and single-layer GNRs were produced after etching for times t_2, t_3, and t_4, respectively ($t_4 > t_3 > t_2 > t_1$; e–g). h) The PMMA was removed to release the GNR. Reproduced with permission from Ref. [64]. Copyright 2009, Nature publishing group.

For persepctive, even though several methods have been reported for the fabrication of GNRs, a workable large-scale production has not yet been achieved. Furthermore, using CNTs as a starting material also means dealing with many or all of the drawbacks that the scientists working with CNTs are still trying to solve. Finally, all of the top-down syntheses of GNRs fail to provide reliable control over the edges of the resulting nanoribbons, and the synthesis of GNRs with widths below 5 nm seems to be limited by the current state-of-the-art lithography techniques.

2.4. Synthesis of Nanographene

Nanographene (with a size between 1 and 100 nm) can serve as a model system for graphene studies. There have been few methods to obtain nanographene with less-defined structures. As early as in 2001, single-layer nanographene sheets with a size of approxiamtely 10 nm were prepared through heat-induced conversion of nanodiamond particles on HOPG.[65] The structure of the obtained nanographenes was visualized at the atomic level by means of scanning tunneling microscopy (STM). Later, electrophoretic deposition of diamond nanoparticles yielded single-layer GNRs with a width of approximately 8 nm, the structure of which was determined by resonance Raman experiments.[66] These studies were conducted just before the reported discovery of graphene in 2004.

More recently, geometrically well-defined graphene quantum dots (GQDs) were produced based on the cage opening of C_{60} on a ruthenium surface. In this process, the strong C_{60}–ruthenium interaction induces the formation of surface vacancies in the ruthenium single crystal and a subsequent embedding of C_{60} molecules on the surface. At elevated temperatures, the embedded C_{60} molecules produce carbon clusters that undergo diffusion and aggregation to form GQDs with perfect hexagonal shapes (5 nm in size) in approximately 30% yield.[67] Graphene oxide and graphite have also been utilized to create small graphene fragments, such as nanographene oxide and graphene dots, which show wavelength-dependent emission behavior. They are promising for applications in photovoltaic devices, cellular imaging, and drug delivery.[68] Nevertheless, these nanographene species have poorly defined structures, and the fundamental mechanisms of their fluorescence properties upon surface passivation are still unclear.

3. Bottom-Up Synthesis of Nanographenes

3.1. Synthesis of Graphene Molecules

As noted above, the top-down methods for graphene synthesis seem to suffer from drawbacks such as uncontrollable sizes and irregular edge structures. In contrast, a bottom-up organic synthesis approach has been developed which may serve as an indispensable tool to create structurally defined graphenes. In this context, our group has been devoted to the atomically precise synthesis of nanographenes and GNRs for decades. Nanographenes and GNRs of various sizes and shapes have been obtained in bulk scale, thus offering an opportunity for the additional solution/vacuum processing and device fabrication.[69]

The bottom-up synthesis of graphenes was initiated through the versatile organic chemistry of PAHs. According to the definition given in the introduction, graphene molecules with a size between 1 and 5 nm can be considered as the smallest nanographene. By far, the largest synthesized monodisperse nanographene molecule consists of 222 carbon atoms with a disk diameter of 3.2 nm, while one of the smallest and most frequently investigated graphene mole-

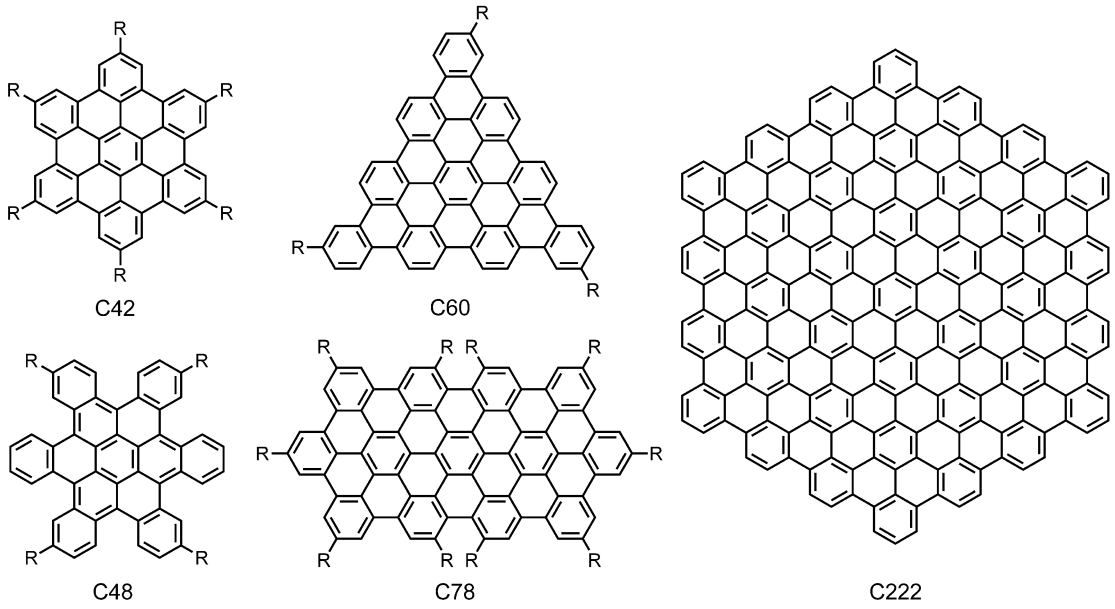

Scheme 1. Chemical structures of several large graphene molecules.

cules, hexa-*peri*-hexabenzocoronene (HBC), has a size of approximately 1.4 nm (Scheme 1).[70]

Similar to graphene, unsubstituted graphene molecules are only sparingly soluble in common organic solvents. To make these materials processable for device fabrication, one has to introduce solubilizing alkyl chains attached to the periphery of the molecule. In this respect, functionalized graphene molecules can also exhibit distinct phase-forming behavior.[71] Flexible substituents can increase the overall disorder and lead to the self-assembly of graphene molecules in the solid state to build up highly ordered columnar superstructures. This is a typical feature for discotic liquid crystals. In addition, graphene molecules with suitable substituents can self-assemble into nanofiber or nanotube architectures in solution, as well as on the surface or at the liquid-solid interface with patterned nanostructures.[72] The solution and vacuum deposition of graphene molecules on the surface enables the identification and manipulation of a single nanographene object, an obvious advantage in comparison to a graphene sheet.[73]

The early syntheses of graphene molecules started from the pioneering contributions by the groups of E. Clar and R. Scholl at the beginning of the last century.[74] Subsequently, more efficient and milder synthetic protocols as well as characterization techniques have been developed, thus leading to the expansion of the family of graphene molecules.[23b,25] Typically, large dendritic oligophenylene precursors of various sizes and shapes were first obtained by means of the Diels–Alder reaction[75] or cyclotrimerization of suitable acetylene building blocks. Intramolecular cyclodehydrogenation[76] and planarization of the resulting precursors, using Lewis oxidants/acids (e.g $FeCl_3$, $AlCl_3/Cu(OTf)_2$), generate large benzenoid graphene molecules of different molecular sizes, symmetries, and edge peripheries. For instance, flat graphene molecules having a triangular shape (C60), a linear ribbon shape (C78), as well as other geometries have been attainable through this approach (Scheme 1).[70] Using a photoinduced cyclodehydrogenation of stilbene-type precursors, Nuckolls et al. succeeded in the synthesis of the hexa-*cata*-hexabenzocoronene (C48) with the aromatic core distorted away from planarity by the steric congestion of its proximal carbon atoms. Graphene molecules fused with additional double bonds, which act as zigzag edges, have also been produced.[77] This approach can provide a powerful means to tune the optoelectronic properties of graphene molecules.[77b] In addition, the incorporation of heteroatoms such as sulphur and nitrogen into the graphene frameworks enables one to tune their optoelectronic properties without changing the conjugated skeleton.[78] Thereby, in stark contrast to graphenes prepared from top-down strategies, the bottom-up chemical approach offers a great opportunity to tailor the molecular size, shape, edge, and composition of graphenes.

Despite the obvious appeal of accessing increasingly large, yet structurally well-defined models of graphene, the concept of planarizing large oligophenylene precursors unfortunately reaches its limit in solution. This is primarily caused by poor solubility of precursors, as well as a mismatching of topology for large oligophenylene precursors, thus leading to partial cyclodehydrogenation. For instance, planarization of a C474 oligophenylene (ca. 4.8 nm) dendrimer yielded only a mixture of completely fused product and partially fused three-dimensional (3D) propeller-shaped molecules.[79] In addition, the exact structural characterization of the products become increasingly difficult given the strong aggregation and profound insolubility of the giant graphene molecules.

3.2. Solution Synthesis of Graphene Nanoribbons

The protocol employed for the synthesis of graphene molecules can be additionally elaborated to build GNRs from one-dimensional (1D) linear polyphenylene precursors. Here,

the critical issue is to achieve high-molecular-weight precursor polymers, which can eventually deliver GNRs with a large aspect ratio. Recently, a homologous series of five monodisperse linear polyphenylenes **1**, having rigid dibenzo[*e*,*l*]pyrene cores in the repeating units, was built through a stoichiometrically controlled, microwave-assisted Diels–Alder reaction (Scheme 2).[20b] The obtained polyphenylene precursors range from 132 ($n=1$) to 372 ($n=5$) carbon atoms in the aromatic backbone by incorporating up to six dibenzo[*e*,*l*]pyrene units. Subsequent cyclodehydrogenation of the polyphenylenes **1** afforded the planarized ribbon **2**. The lowest homologue **2a**, containing 132 carbon atoms in the aromatic core, was sufficiently soluble to be fully characterized, whereas characterization of the higher homologues of these planarized molecules (**2b**–**e**) was hampered because of their low solubility.[20b]

Another type of linear GNRs, **4**, was achieved by oxidative cyclodehydrogenation of the hexaphenylbenzene-type polymers **3** prepared by Suzuki polymerization (Scheme 3).[20a,80] Comparison of the MALDI-TOF spectra between the precursor **3** and product **4** demonstrated that the Scholl reaction of polyphenylene precursors proceeds smoothly. The presence of branched alkyl chains located at adjacent positions of the aromatic periphery makes the resulting GNRs **4** quite soluble in common organic solvents, and additionally suppresses aggregation in solution.[81] As a result, UV/Vis absorption spectroscopy and scanning tunneling microscopy (STM) can be used to characterize the nanoribbons **4** having lengths of up to 12 nm, thus confirming the complete cyclodehydrogenation of the polyphenylene precursor **3**.

The above synthetic protocols have limitations in terms of the length of the resulting ribbons. The main drawback is the strong aggregation of rigid polyphenylene backbones, thus limiting the solubility of the precursors in the polymerization step. To overcome this obstacle, nanoribbons **8**–**10** having a kinked polyphenylene backbone were recently designed (Scheme 4).[20f] This strategy led to a significantly increased solubility of poly(*o*-phenylene-*p*-phenylene) systems. The precursors **5**–**7** can be prepared by microwave-assisted Suzuki polycondensation of *ortho*-dibromobenzenes and benzene-1,4-diboronic esters. For example, for the polymer **6** having solubilizing dodecyl chains and a molecular weight of up to 20000 g mol^{-1} was detected by MALDI-TOF MS, and gel permeation chromatography (GPC) analysis with polystyrene (PS) standards indicated an number-average molecular weight of $M_n = 9900$ g mol^{-1} and a polydispersity index (PDI) as low as 1.40. Thereby, full dehydrogenation of polyphenylene with a length of more than 40 nm is possible through a $FeCl_3$-mediated Scholl reaction. The resulting nanoribbon **9** is soluble in common organic solvents, thus making further structural characterizations and processing of GNRs possible.

Despite the progress achieved in the bottom-up organic synthesis of graphenes by wet chemical means, several drawbacks still need to be resolved. For example, the final and vital step of "graphenization", that is, the transformation of a 3D polyphenlene precursor into a rigid, planar aromatic is far from established reactions. Photoinduced cyclodehy-

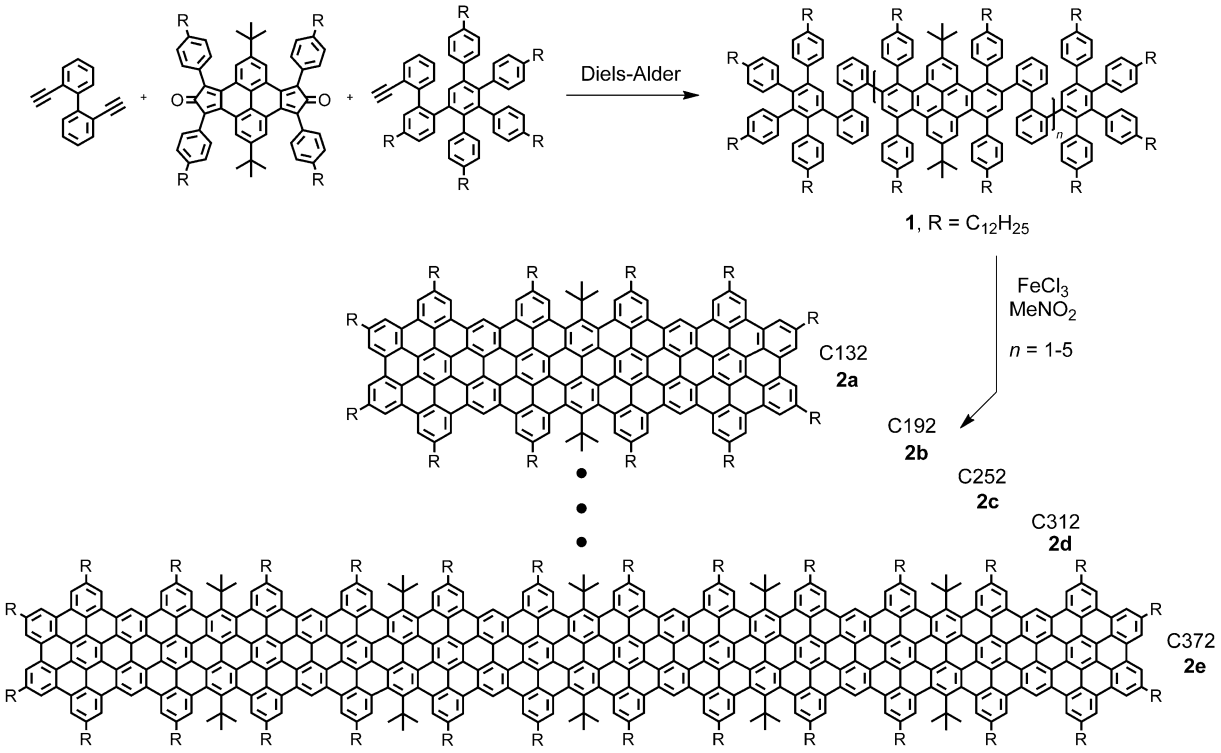

Scheme 2. Syntheis of monodisperse ribbon-type polyphenylenes **1** and subsequent cyclodehydrogenated nanoribbons **2a**–**e**. Modified with permission from Ref. [20b], Copyright 2009, American Chemical Society.

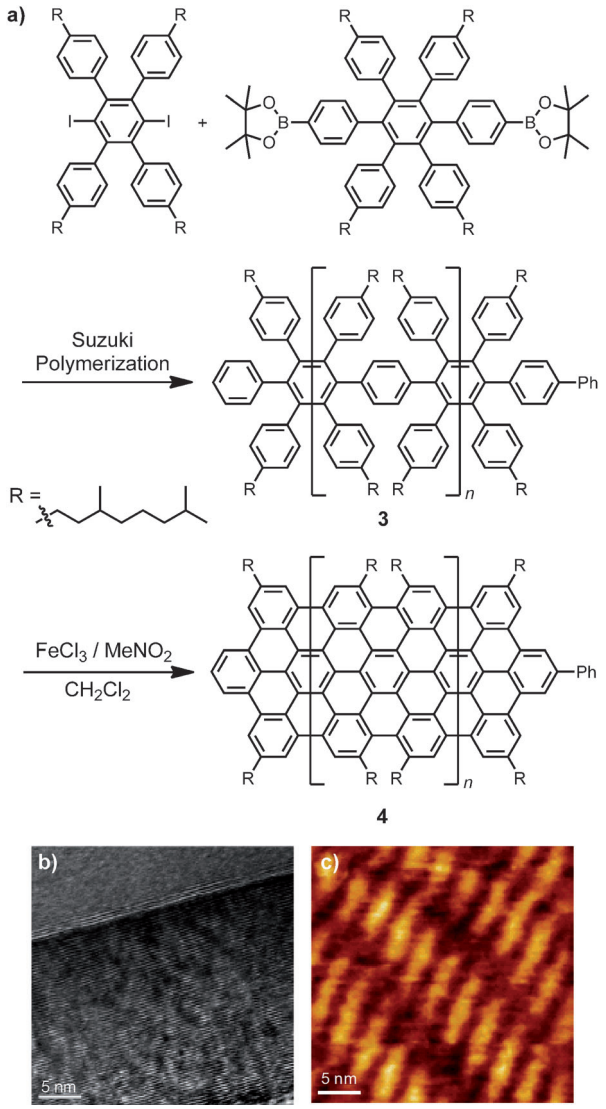

Scheme 3. a) Synthesis of soluble GNRs **4**. b) HRTEM of GNRs **4**. c) STM image of GNRs **4** at the solid/liquid interface on HOPG. Modified with permission from Ref. [20a], Copyright 2008, American Chemical Society.

drogenation seems to be only efficient for small stilbene-type precursors.[82] Other commonly used intramolecular oxidative cyclodehydrogenations under Scholl reaction conditions (Lewis acids/oxidants) suffer from intrinsic problems of reactivity and regioselectivity. Not every polyphenylene precursor can be graphenized because of incomplete reactions,[83] unexpected migrations/rearrangements of precursors,[84] or lack of regioselectivity.[20f,85] Different substitution and steric hindrance of the precursors also make the intramolecular Scholl reaction less predictable. Therefore, alternative methods need to be sought, such as modern transition-metal-catalyzed cross-coupling reactions applicable for aryl–aryl bond formation. Such new approaches may offer routes for the construction of even larger graphene-like systems.

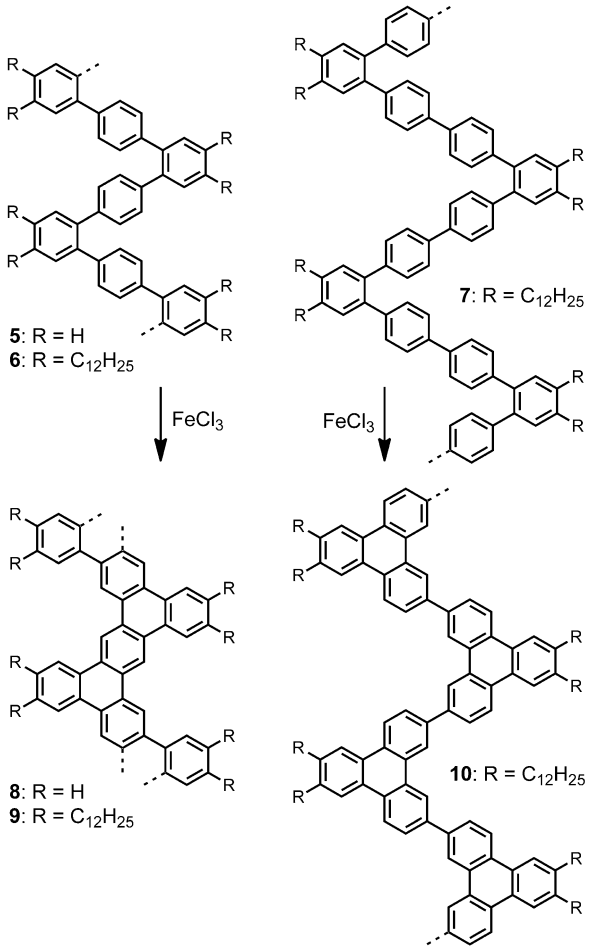

Scheme 4. Synthesis of soluble nanoribbons **8**–**10** with a kinked conjugated backbone. Modified with permission from Ref. [20c], Copyright 2011, Wiley-VCH.

3.3. Surface-Mediated Synthesis of Nanographene and Graphene Nanoribbons

The cyclodehydrogenation reactions for graphene synthesis presented in the last section are typically carried out in solution, thus making the solubility of oligophenylene precursors and their compatibility with reaction conditions crucial parameters. In contrast, graphene molecules and graphene nanoribbons with and extended aromatic core always suffer from strong intermolecular π–π stacking and poor solubility in conventional organic solvents, which make solution processing for electronic device applications difficult. The thermal evaporation of either these molecules or ribbons is generally difficult in view of their size. To surmount these obstacles, on-surface covalent synthesis routes would serve as a powerful alternative for the bottom-up creation of graphene structures. Actually, the surface-mediated syntheses of planar PAHs from oligophenylene precursors were studied at liquid-solid interface to some extent before the graphene era,[86] although no detailed investigations of these reactions have been reported. Very recently, the surface-mediated synthesis of graphene has been proposed under ultrahigh vacuum (UHV) conditions.[21] In this approach, molecular layers of

oligophenylene precursors are first deposited onto a suitable metallic surface and then subjected to thermal-assisted polymerization and cyclodehydrogenation, eventually producing the desired graphene product. By using such an approach, direct access to nanographenes and graphene nanoribbons on a surface from pre-deposited precursors may facilitate their introduction in electronic devices.

3.3.1. Surface-Mediated Synthesis of Nanographene

As the first step towards controlling graphene synthesis on surfaces, Fasel, Müllen, and co-workers found that cyclodehydrogenation of nonplanar polyphenylene precursors could be thermally induced on Cu(111) (Figure 8).[21f] By

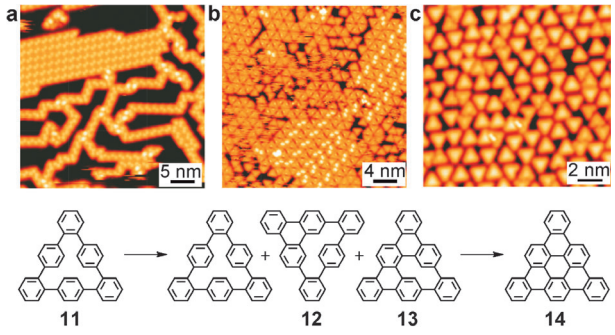

Figure 8. STM images of the cyclodehydrogenation of **11** on Cu(111). a) Self-assembled structures after deposition at room temperature. b) Co-existence of **11**, intermediates **12**, **13**, and the final product **14** after heating at ca. 450 K. c) Sample after annealing at ca. 470 K showing the final PAH **14**. Modified with permission from Ref. [21f], Copyright 2011, Nature publishing group.

using low-temperature STM and ab initio simulations, it was noted that the thermally activated cyclodehydrogenation of cyclohexa-*o*-*p*-*o*-*p*-*o*-*p*-phenylene (**11**) proceeded in six consecutive steps through five intermediates, thus leading to the completely planar nanographene **14**. Compared to thermally induced intramolecular cyclodehydrogenation under flash vacuum pyrolysis (FAP) conditions,[87] the required reaction temperature in the present case was significantly lower (ca. 200 °C). This lower temperature is a result of two major driving forces of the reaction: 1) the catalytically activated solvation of hydrogen atoms by the substrate and 2) the van der Waals interactions between molecules and substrate, thus increasing the overall intramolecular strain and weakening the C–H bonds. The corresponding mechanisms identified here should be also applicable for surface-assisted dehydrogenative aryl–aryl coupling reactions in many other molecule-substrate systems. Although the cyclodehydrogenation reaction was performed in particular on Cu(111), a hybrid simulation suggested that the reaction should also work on other substrate, such as passivated semiconductor surfaces.

3.3.2. Surface-Mediated Synthesis of GNRs

Apart from surface-mediated intramolecular cyclodehydrogenation of oligophenylene precursors, the concept of a surface synthesis approach has been found to be exceptionally useful for the polymerization of aromatic precursors with halogen groups (such as bromo or iodo substituents) on their peripheries.[88] The rational combination of these two types of reactions has led to the successful synthesis of atomically precise GNRs based on dihalogenated oligophenylene monomers.[21a] Figure 9 illustrates the basic fabrication steps of such

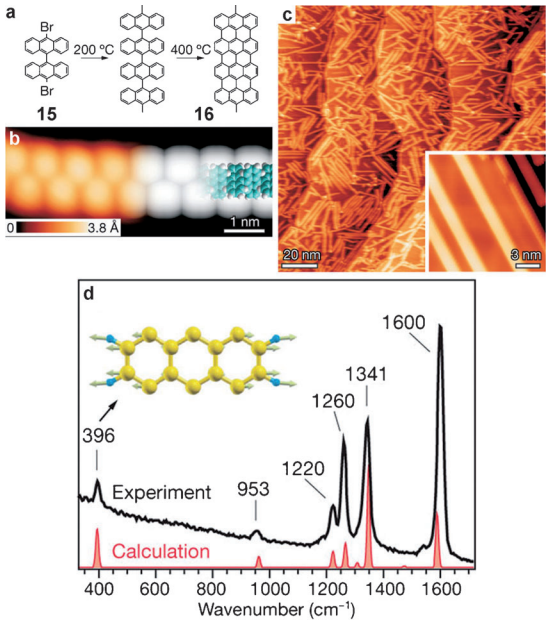

Figure 9. Straight GNRs from bianthryl monomers. a) Reaction scheme for conversion of **15** to **16**. b) STM image taken after suface-assisted C–C coupling at 200 °C and DFT-based simulation of the STM image (right) with partly overlaid model of the polymer. c) Overview STM image after cyclodehydrogenation at 400 °C. d) Raman spectrum of straight $N = 7$ GNRs. (N refers to the number of carbon atoms along the direction of short axis.) Reproduced with permission from Ref. [21a]. Copyright 2010, Nature publishing group.

nanoribbons obtained from 10,10′-dibromo-9,9′-bianthryl (**15**) monomers.[89] The first thermal activation step of an assembled monolayer of **15** on metal surfaces such as Ag(111) or Au(111) at 200 °C cleaves the halogen substituents, thus yielding surface-stabilized biradical species which undergo Ullmann type aryl–aryl coupling reactions[90] to form linear polymer chains. Subsequent annealing of the sample at 400 °C induces intramolecular cyclodehydrogenation and planarization of the polymer chain and hence the formation of a straight ribbon **16** with an armchair edge. Raman spectroscopy of the graphene nanoribbons (Figure 9d) exhibit, in addition to the G and D bands characteristic for all carbon-based materials (at 1600 and 1341 cm^{-1}, respectively), specific edge modes that are absent in pristine graphene. A transfer method of GNR **16** from the gold surface to silicon dioxide substrate has also been demonstrated by a polydimethylsiloxane (PDMS) stamp transfer process with subsequent etching of the gold layer in KI solution.

As the topology of GNRs is exclusively determined by the precursor monomers utilized, one can expect that the abundant availability of different halogenated oligopheny-

lene precursors will allow the synthesis of GNRs with different architectures. For instance, a chevron-type GNR with a periodicity of 1.70 nm and pure armchair edge structure was obtained by using 6,11-dibromo-1,2,3,4-tetraphenyltriphenylene (**17**) as the precursor monomer (Figure 10 a,b). Most of the GNRs show a length of 20–30 nm and in a few cases up to 100 nm. Moreover, by adding one more C_3-symmetric triiodo-functionalized monomer, 1,3,5-tris(4″-iodo-2′-biphenyl)benzene **19**, to **17** (Figure 10 c), a threefold GNR junction could be produced (Figure 10 c,d).

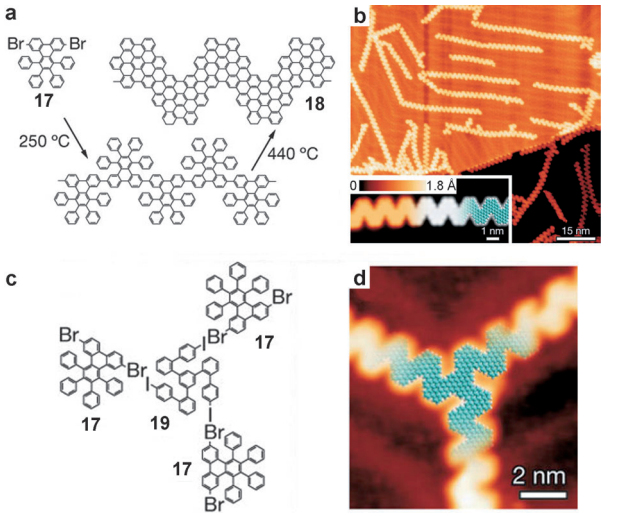

Figure 10. Chevron-type GNRs from tethraphenyl-triphenylene monomers. a) Reaction scheme for converison of **17** into chevron-type GNRs. b) Overview STM image of chevron-tpye GNRs fabricated on a Au(111) surface. Inset: High-resolution STM image and DFT-based simulation of the STM image (greyscale) with partly overlaid molecular model of the ribbon. c) Schematic model of the junction fabrication process with components **19** and **17**. d) Model (blue C; white H) of the colligated and dehydrogenated molecules forming the threefold junction overlaid on the STM image. Reproduced with permission from from Ref. [21a]. Copyright 2010, Nature publishing group.

3.3.3. Surface-Mediated Synthesis of Porous Graphene

Certainly, the use of surface-mediated polymer formation should be expandable to the controlled synthesis of graphene into two dimensions. In this way, one should be able to tailor the structure, composition and electronic properties of graphene sheets at the molecular level, a level of control which has yet to be accessed by other top-down or bottom-up methods. To achieve this goal, oligophenylene precursors with multiple reactive sites on a surface are required. Upon our first attempt, a periodically ordered porous graphene network with atomic precision was built up based on a surface-mediated Ullmann-type coupling of a specially designed hexaiodo-cyclohexa-*m*-phenylene (CHP; Figure 11 a).[21g] A highly regular honeycomb graphene network was prepared by thermal annealing of CHP on Ag(111) at 575 K for 5 minutes, for which STM images clearly reveal a pore spacing of 7.4 Å (Figure 11 b,c). However, the domain size of the produced porous graphene is so far mostly limited to 50 nm × 50 nm. This spacing is probably due to the low surface mobility and

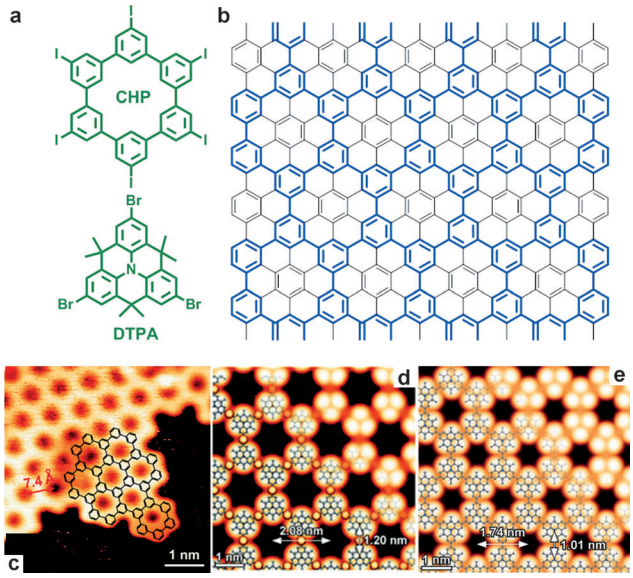

Figure 11. a) Structure of CHP and DTPA. b) Structural relationship of the polyphenylene superhoneycomb network (blue lines) and graphene. c) High-resolution STM image of an edge of the porous graphene network based on CHP. d, e) Model and STM simulation of a coordination polymer with Ag atoms and covalent network based on DTPA, respectively. Images b) and c) modified with permission.[21g] Copyright 2008, Royal Society of Chemistry. Images d) and e) reproduced with permission from Ref. [92]. Copyright 2011, Royal Society of Chemistry)

reactivity of large precursors on the surface and the grain boundaries of the metallic substrate. In addition, the nature of the metal surfaces, such as Au(111), Ag(111), and Cu(111), also influences the efficiency of C–C bond formations.[91]

Recently, Fasel, Müllen, and co-workers reported another example of a porous graphene network based on the on-surface polymerization of tribromo-substituted dimethylmethylene-bridged triphenylamine (heterotriangulene, DTPA, Figure 11 a) on Ag(111).[92] A coordination polymer was first formed by treatment of DPTA at 200 °C. Upon elevating the surface temperature to 300 °C, a proper 2D covalent polymer network could be established, accompanied by the reduction of pore spacing from 2.1 to 1.7 nm (Figure 11 d,e). Further heat treatment at 400 °C selectively cleaved the methyl units, thus resulting in a flat covalent framework. As the electron-rich nitrogen atoms are periodically incorporated into such porous graphene network, oxidation of N may generate stable radical cations and provide an opportunity for the creation of complexes extending into the third dimension.

4. Conclusions and Perspectives

Carbon allotropes such as graphene and carbon nanotubes have, in recent years, been developed from basic research to prospective applications. However, several challenges for their controllable production are yet to be addressed. In the case of graphene, chemical strategies are in our opinion the most promising way towards the controlled

synthesis of graphene nanostructures spanning from graphene sheets and graphene nanoribbons to nanographenes.

Top-down approaches that use graphite as a precursor towards the production of graphene have taken advantage of exfoliation and stabilization mechanisms in the liquid phase. However, the use of high-boiling and strongly polar organic solvents seems to be a limiting factor, thus precluding exfoliated graphene from practical electronic device fabrication. Therefore, an unresolved issue is the development of facile and reproducible means by which to prepare high quality graphene on large scale and with good solution processability. Graphene grown by CVD has already found its way into many functional devices, however several factors are yet to be optimized, including the production of large-area crystals and their clean and cost-efficient transfer onto insulating/bendable substrates.

To reliably introduce a band gap in graphene, cutting it into narrow strips, that is GNRs, constitutes the most straightforward way. Despite recent advances in synthesis of GNRs by both top-down and bottom-up means, several challenges remain for the chemical synthesis before one can truly realize their applications in electronics. As a first step, GNRs with low band gaps (0.1–1 eV) are desired and thus controlled synthesis of GNRs with widths of 2–5 nm needs to be unraveled. Longer GNRs with lengths comparable to their analogue CNTs on a micrometer scale are preferred to make the physical characterization and device fabrication simpler. In addition, GNRs fabricated to date mainly show armchair or undefined edges, while GNRs with pure zigzag edges remain an unexplored synthetic target. Importantly, the latter has been predicated to possess metallic features and to be useful for spin electronics.[93]

For the bottom-up solution synthesis of graphene nanostructures, numerous high-molecular-weight oligophenylene precursors are synthetically available. However, to obtain access to expanded nanographenes and GNRs with defined structures, the drawbacks of the intramolecular cyclodehydrogenation must be overcome. Similar to graphene, additional processing is indispensible to making large nanographenes and GNRs useful for electronic devices. Conversely, the recent advances in surface-mediated synthesis have led to the structural control of graphenes at atomic precision. One can certainly expand the collection of graphene structures having defined geometry and edge periphery by taking advantage of available synthetic tools. Nevertheless, restrictions such as the use of ultra-high vacuum (UHV) systems and single-crystalline conducting substrates should be avoided in the future. Thus, developing a non-UHV system, like the well-established CVD technique, for surface synthesis of GNRs is the next target. The growth of GNRs with ordered alignment will be another important direction.

The encouraging results of the current chemical synthesis of graphene materials have already determined the direction of future research efforts. Chemists and material scientists are developing reliable solution and surface synthesis approaches based on both top-down and bottom-up strategies which yield defect-free graphene structures with tailored properties. They are also developing synthetic and processing protocols which can be performed under conditions compatible with standard metal-oxide-semiconductor (CMOS) fabrication processes. Once these challenges have been mastered, the industrial production of graphene-based electronics will become reality.

We gratefully acknowledge the financial support by the Max Planck Society through the program ENERCHEM, DFG Priority Program SPP 1355, DFG Priority Program SPP 1459, BMBF LiBZ Project, BMBF Graphenoid Project, ESF Project GOSPEL (Ref Nr: 09-EuroGRAPHENE-FP-001), FP7-Energy-2010-FET Project Molesol, EU Project GENIUS, and ERC grant on NANOGRAPH.

Received: February 8, 2012
Published online: July 6, 2012

[1] H. W. Kroto, J. R. Heath, S. C. O'Brien, R. F. Curl, R. E. Smalley, *Nature* **1985**, *318*, 162 – 163.
[2] S. Iijima, *Nature* **1991**, *354*, 56 – 58.
[3] a) G. Otero, G. Biddau, C. Sanchez-Sanchez, R. Caillard, M. F. Lopez, C. Rogero, F. J. Palomares, N. Cabello, M. A. Basanta, J. Ortega, J. Mendez, A. M. Echavarren, R. Perez, B. Gomez-Lor, J. A. Martin-Gago, *Nature* **2008**, *454*, 865 – 868; b) L. T. Scott, M. M. Boorum, B. J. McMahon, S. Hagen, J. Mack, J. Blank, H. Wegner, A. de Meijere, *Science* **2002**, *295*, 1500 – 1503.
[4] K. S. Novoselov, A. K. Geim, S. V. Morozov, D. Jiang, Y. Zhang, S. V. Dubonos, I. V. Grigorieva, A. A. Firsov, *Science* **2004**, *306*, 666 – 669.
[5] a) A. K. Geim, *Angew. Chem.* **2011**, *123*, 7100 – 7122; *Angew. Chem. Int. Ed.* **2011**, *50*, 6966 – 6985; b) K. S. Novoselov, *Angew. Chem.* **2011**, *123*, 7123 – 7141; *Angew. Chem. Int. Ed.* **2011**, *50*, 6986 – 7002.
[6] a) K. S. Novoselov, A. K. Geim, S. V. Morozov, D. Jiang, M. I. Katsnelson, I. V. Grigorieva, S. V. Dubonos, A. A. Firsov, *Nature* **2005**, *438*, 197 – 200; b) R. M. Westervelt, *Science* **2008**, *320*, 324 – 325; c) S. V. Morozov, K. S. Novoselov, M. I. Katsnelson, F. Schedin, D. C. Elias, J. A. Jaszczak, A. K. Geim, *Phys. Rev. Lett.* **2008**, *100*, 016602.
[7] a) F. Schedin, A. K. Geim, S. V. Morozov, E. W. Hill, P. Blake, M. I. Katsnelson, K. S. Novoselov, *Nat. Mater.* **2007**, *6*, 652 – 655; b) V. Dua, S. P. Surwade, S. Ammu, S. R. Agnihotra, S. Jain, K. E. Roberts, S. Park, R. S. Ruoff, S. K. Manohar, *Angew. Chem.* **2010**, *122*, 2200 – 2203; *Angew. Chem. Int. Ed.* **2010**, *49*, 2154 – 2157.
[8] a) D. R. Dreyer, C. W. Bielawski, *Chem. Sci.* **2011**, *2*, 1233 – 1240; b) G. M. Scheuermann, L. Rumi, P. Steurer, W. Bannwarth, R. Mulhaupt, *J. Am. Chem. Soc.* **2009**, *131*, 8262 – 8270.
[9] a) M. Pumera, *Energy Environ. Sci.* **2011**, *4*, 668 – 674; b) Y. Sun, Q. Wu, G. Shi, *Energy Environ. Sci.* **2011**, *4*, 1113 – 1132.
[10] M. D. Stoller, S. Park, Y. Zhu, J. An, R. S. Ruoff, *Nano Lett.* **2008**, *8*, 3498 – 3502.
[11] W. R. Yang, K. R. Ratinac, S. P. Ringer, P. Thordarson, J. J. Gooding, F. Braet, *Angew. Chem.* **2010**, *122*, 2160 – 2185; *Angew. Chem. Int. Ed.* **2010**, *49*, 2114 – 2138.
[12] P. Avouris, *Nano Lett.* **2010**, *10*, 4285 – 4294.
[13] R. Ruoff, *Nat. Nanotechnol.* **2008**, *3*, 10 – 11.
[14] Y.-M. Lin, C. Dimitrakopoulos, K. A. Jenkins, D. B. Farmer, H.-Y. Chiu, A. Grill, P. Avouris, *Science* **2010**, *327*, 662.
[15] J. M. Englert, A. Hirsch, X. L. Feng, K. Müllen, *Angew. Chem.* **2011**, *123*, A17 – A24; *Angew. Chem. Int. Ed.* **2011**, *50*, A17 – A24.
[16] X. Li, X. Wang, L. Zhang, S. Lee, H. Dai, *Science* **2008**, *319*, 1229 – 1232.
[17] a) W. S. Hummers, R. E. Offeman, *J. Am. Chem. Soc.* **1958**, *80*, 1339 – 1339; b) S. Stankovich, D. A. Dikin, G. H. B. Dommett,

K. M. Kohlhaas, E. J. Zimney, E. A. Stach, R. D. Piner, S. T. Nguyen, R. S. Ruoff, *Nature* **2006**, *442*, 282 – 286; c) D. Li, M. B. Muller, S. Gilje, R. B. Kaner, G. G. Wallace, *Nat. Nanotechnol.* **2008**, *3*, 101 – 105; d) V. C. Tung, M. J. Allen, Y. Yang, R. B. Kaner, *Nat. Nanotechnol.* **2009**, *4*, 25 – 29.

[18] a) C. Berger, Z. Song, X. Li, X. Wu, N. Brown, C. Naud, D. Mayou, T. Li, J. Hass, A. N. Marchenkov, E. H. Conrad, P. N. First, W. A. de Heer, *Science* **2006**, *312*, 1191 – 1196; b) P. W. Sutter, J.-I. Flege, E. A. Sutter, *Nat. Mater.* **2008**, *7*, 406 – 411.

[19] C. Berger, Z. Song, T. Li, X. Li, A. Y. Ogbazghi, R. Feng, Z. Dai, A. N. Marchenkov, E. H. Conrad, P. N. First, W. A. deHeer, *J. Phys. Chem. B* **2004**, *108*, 19912 – 19916.

[20] a) X. Yang, X. Dou, A. Rouhanipour, L. Zhi, H. J. Räder, K. Müllen, *J. Am. Chem. Soc.* **2008**, *130*, 4216 – 4217; b) Y. Fogel, L. Zhi, A. Rouhanipour, D. Andrienko, H. J. Räder, K. Müllen, *Macromolecules* **2009**, *42*, 6878 – 6884; c) L. Dössel, L. Gherghel, X. Feng, K. Müllen, *Angew. Chem.* **2011**, *123*, 2588 – 2591; *Angew. Chem. Int. Ed.* **2011**, *50*, 2540 – 2543.

[21] a) J. Cai, P. Ruffieux, R. Jaafar, M. Bieri, T. Braun, S. Blankenburg, M. Muoth, A. P. Seitsonen, M. Saleh, X. Feng, K. Müllen, R. Fasel, *Nature* **2010**, *466*, 470 – 473; b) M. S. Fuhrer, *Nat. Mater.* **2010**, *9*, 611 – 612; c) J. Björk, S. Stafström, F. Hanke, *J. Am. Chem. Soc.* **2011**, *133*, 14884 – 14887; d) C.-A. Palma, P. Samori, *Nat. Chem.* **2011**, *3*, 431 – 436; e) J. A. Martin-Gago, *Nat. Chem.* **2011**, *3*, 11 – 12; f) M. Treier, C. A. Pignedoli, T. Laino, R. Rieger, K. Müllen, D. Passerone, R. Fasel, *Nat. Chem.* **2011**, *3*, 61 – 67; g) M. Bieri, M. Treier, J. Cai, K. Ait-Mansour, P. Ruffieux, O. Groning, P. Groning, M. Kastler, R. Rieger, X. Feng, K. Müllen, R. Fasel, *Chem. Commun.* **2009**, 6919 – 6921.

[22] a) S. Pang, Y. Hernandez, X. Feng, K. Müllen, *Adv. Mater.* **2011**, *23*, 2779 – 2795; b) D. Q. Wu, F. Zhang, P. Liu, X. L. Feng, *Chem. Eur. J.* **2011**, *17*, 10804 – 10812; c) D. R. Dreyer, R. S. Ruoff, C. W. Bielawski, *Angew. Chem.* **2010**, *122*, 9524 – 9532; *Angew. Chem. Int. Ed.* **2010**, *49*, 9336 – 9344.

[23] a) A. Naeemi, J. D. Meindl, *Ieee Electron Device Lett.* **2007**, *28*, 428 – 431; b) D. S. L. Abergel, V. Apalkov, J. Berashevich, K. Ziegler, T. Chakraborty, *Adv. Phys.* **2010**, *59*, 261 – 482; c) A. H. Castro Neto, F. Guinea, N. M. R. Peres, K. S. Novoselov, A. K. Geim, *Rev. Mod. Phys.* **2009**, *81*, 109 – 162.

[24] *A Guide to IUPAC Nomenclature of Organic Compounds*, Blackwell Scientific Publications, London, **1997**.

[25] L. Zhi, K. Müllen, *J. Mater. Chem.* **2008**, *18*, 1472 – 1484.

[26] Y. Hernandez, V. Nicolosi, M. Lotya, F. M. Blighe, Z. Sun, S. De, I. T. McGovern, B. Holland, M. Byrne, Y. K. Gun'Ko, J. J. Boland, P. Niraj, G. Duesberg, S. Krishnamurthy, R. Goodhue, J. Hutchison, V. Scardaci, A. C. Ferrari, J. N. Coleman, *Nat. Nanotechnol.* **2008**, *3*, 563 – 568.

[27] P. Blake, P. D. Brimicombe, R. R. Nair, T. J. Booth, D. Jiang, F. Schedin, L. A. Ponomarenko, S. V. Morozov, H. F. Gleeson, E. W. Hill, A. K. Geim, K. S. Novoselov, *Nano Lett.* **2008**, *8*, 1704 – 1708.

[28] X. Li, G. Zhang, X. Bai, X. Sun, X. Wang, E. Wang, H. Dai, *Nat. Nanotechnol.* **2008**, *3*, 538 – 542.

[29] C.-J. Shih, A. Vijayaraghavan, R. Krishnan, R. Sharma, J.-H. Han, M.-H. Ham, Z. Jin, S. Lin, G. L. C. Paulus, N. F. Reuel, Q. H. Wang, D. Blankschtein, M. S. Strano, *Nat. Nanotechnol.* **2011**, *6*, 439 – 445.

[30] a) A. Kumar, C. Zhou, *ACS Nano* **2010**, *4*, 11 – 14; b) S. De, P. J. King, M. Lotya, A. O'Neill, E. M. Doherty, Y. Hernandez, G. S. Duesberg, J. N. Coleman, *Small* **2010**, *6*, 458 – 464.

[31] a) M. Lotya, P. J. King, U. Khan, S. De, J. N. Coleman, *ACS Nano* **2010**, *4*, 3155 – 3162; b) M. Lotya, Y. Hernandez, P. J. King, R. J. Smith, V. Nicolosi, L. S. Karlsson, F. M. Blighe, S. De, Z. Wang, I. T. McGovern, G. S. Duesberg, J. N. Coleman, *J. Am. Chem. Soc.* **2009**, *131*, 3611 – 3620; c) S. D. Bergin, V. Nicolosi, H. Cathcart, M. Lotya, D. Rickard, Z. Sun, W. J. Blau, J. N. Coleman, *J. Phys. Chem. C* **2008**, *112*, 972 – 977; d) V. C. Moore, M. S. Strano, E. H. Haroz, R. H. Hauge, R. E. Smalley, J. Schmidt, Y. Talmon, *Nano Lett.* **2003**, *3*, 1379 – 1382; e) M. J. O'Connell, P. Boul, L. M. Ericson, C. Huffman, Y. H. Wang, E. Haroz, C. Kuper, J. Tour, K. D. Ausman, R. E. Smalley, *Chem. Phys. Lett.* **2001**, *342*, 265 – 271.

[32] A. A. Green, M. C. Hersam, *Nano Lett.* **2009**, *9*, 4031 – 4036.

[33] J. M. Englert, J. Röhrl, C. D. Schmidt, R. Graupner, M. Hundhausen, F. Hauke, A. Hirsch, *Adv. Mater.* **2009**, *21*, 4265 – 4269.

[34] a) J.-H. Jang, D. Rangappa, Y.-U. Kwon, I. Honma, *J. Mater. Chem.* **2011**, *21*, 3462 – 3466; b) D. Rangappa, K. Sone, M. Wang, U. K. Gautam, D. Golberg, H. Itoh, M. Ichihara, I. Honma, *Chem. Eur. J.* **2010**, *16*, 6488 – 6494.

[35] E. Widenkvist, et al., *J. Phys. D* **2009**, *42*, 112003.

[36] C. Vallés, C. Drummond, H. Saadaoui, C. A. Furtado, M. He, O. Roubeau, L. Ortolani, M. Monthioux, A. Pénicaud, *J. Am. Chem. Soc.* **2008**, *130*, 15802.

[37] J. M. Englert, C. Dotzer, G. Yang, M. Schmid, C. Papp, J. M. Gottfried, H.-P. Steinrück, E. Spiecker, F. Hauke, A. Hirsch, *Nat. Chem.* **2011**, *3*, 279 – 286.

[38] J. Wang, K. K. Manga, Q. Bao, K. P. Loh, *J. Am. Chem. Soc.* **2011**, *133*, 8888 – 8891.

[39] C.-Y. Su, A.-Y. Lu, Y. Xu, F.-R. Chen, A. N. Khlobystov, L.-J. Li, *ACS Nano* **2011**, *5*, 2332 – 2339.

[40] N. Behabtu, J. R. Lomeda, M. J. Green, A. L. Higginbotham, A. Sinitskii, D. V. Kosynkin, D. Tsentalovich, A. N. G. Parra-Vasquez, J. Schmidt, E. Kesselman, Y. Cohen, Y. Talmon, J. M. Tour, M. Pasquali, *Nat. Nanotechnol.* **2010**, *5*, 406 – 411.

[41] V. León, M. Quintana, M. Antonia Herrero, J. L. G. Fierro, A. de La Hoz, M. Prato, E. Vázquez, *Chem. Commun.* **2011**, *47*, 10936 – 10938.

[42] a) S. Park, R. S. Ruoff, *Nat. Nanotechnol.* **2009**, *4*, 217 – 224; b) Y. Zhu, S. Murali, W. Cai, X. Li, J. W. Suk, J. R. Potts, R. S. Ruoff, *Adv. Mater.* **2010**, *22*, 3906 – 3924; c) D. R. Dreyer, S. Park, C. W. Bielawski, R. S. Ruoff, *Chem. Soc. Rev.* **2010**, *39*, 228 – 240; d) M. J. Allen, V. C. Tung, R. B. Kaner, *Chem. Rev.* **2010**, *110*, 132 – 145.

[43] a) Q. Su, S. P. Pang, V. Alijani, C. Li, X. L. Feng, K. Müllen, *Adv. Mater.* **2009**, *21*, 3191 – 3195; b) Y. Y. Liang, J. Frisch, L. J. Zhi, H. Norouzi-Arasi, X. L. Feng, J. P. Rabe, N. Koch, K. Müllen, *Nanotechnology* **2009**, *20*, 434007.

[44] a) M. Yudasaka, R. Kikuchi, T. Matsui, Y. Ohki, S. Yoshimura, E. Ota, *Appl. Phys. Lett.* **1995**, *67*, 2477 – 2479; b) Z. F. Ren, Z. P. Huang, J. W. Xu, J. H. Wang, P. Bush, M. P. Siegal, P. N. Provencio, *Science* **1998**, *282*, 1105 – 1107; c) G. L. Che, B. B. Lakshmi, E. R. Fisher, C. R. Martin, *Nature* **1998**, *393*, 346 – 349.

[45] K. S. Kim, Y. Zhao, H. Jang, S. Y. Lee, J. M. Kim, K. S. Kim, J. H. Ahn, P. Kim, J. Y. Choi, B. H. Hong, *Nature* **2009**, *457*, 706 – 710.

[46] R. Vitchev, et al., *Nanotechnology* **2010**, *21*, 095602.

[47] S. Marchini, S. Günther, J. Wintterlin, *Phys. Rev. B* **2007**, *76*, 075429.

[48] A. Reina, X. Jia, J. Ho, D. Nezich, H. Son, V. Bulovic, M. S. Dresselhaus, J. Kong, *Nano Lett.* **2009**, *9*, 30 – 35.

[49] D. Wei, Y. Liu, Y. Wang, H. Zhang, L. Huang, G. Yu, *Nano Lett.* **2009**, *9*, 1752 – 1758.

[50] X. S. Li, W. W. Cai, J. H. An, S. Kim, J. Nah, D. X. Yang, R. Piner, A. Velamakanni, I. Jung, E. Tutuc, S. K. Banerjee, L. Colombo, R. S. Ruoff, *Science* **2009**, *324*, 1312 – 1314.

[51] S. Bae, H. Kim, Y. Lee, X. Xu, J.-S. Park, Y. Zheng, J. Balakrishnan, T. Lei, H. Ri Kim, Y. I. Song, Y.-J. Kim, K. S. Kim, B. Ozyilmaz, J.-H. Ahn, B. H. Hong, S. Iijima, *Nat. Nanotechnol.* **2010**, *5*, 574 – 578.

[52] X. Li, C. W. Magnuson, A. Venugopal, R. M. Tromp, J. B. Hannon, E. M. Vogel, L. Colombo, R. S. Ruoff, *J. Am. Chem. Soc.* **2011**, *133*, 2816 – 2819.

[53] X. S. Li, W. W. Cai, L. Colombo, R. S. Ruoff, *Nano Lett.* **2009**, *9*, 4268 – 4272.

[54] Z. Sun, Z. Yan, J. Yao, E. Beitler, Y. Zhu, J. M. Tour, *Nature* **2010**, *468*, 549 – 552.
[55] J. Chen, Y. Wen, Y. Guo, B. Wu, L. Huang, Y. Xue, D. Geng, D. Wang, G. Yu, Y. Liu, *J. Am. Chem. Soc.* **2011**, *133*, 17548 – 17551.
[56] a) C. Mattevi, H. Kim, M. Chhowalla, *J. Mater. Chem.* **2011**, *21*, 3324 – 3334; b) J. M. Wofford, S. Nie, K. F. McCarty, N. C. Bartelt, O. D. Dubon, *Nano Lett.* **2010**, *10*, 4890 – 4896.
[57] a) T. Ohta, A. Bostwick, T. Seyller, K. Horn, E. Rotenberg, *Science* **2006**, *313*, 951 – 954; b) Y. B. Zhang, T. T. Tang, C. Girit, Z. Hao, M. C. Martin, A. Zettl, M. F. Crommie, Y. R. Shen, F. Wang, *Nature* **2009**, *459*, 820 – 823.
[58] M. Y. Han, B. Özyilmaz, Y. Zhang, P. Kim, *Phys. Rev. Lett.* **2007**, *98*, 206805.
[59] J. Bai, X. Duan, Y. Huang, *Nano Lett.* **2009**, *9*, 2083 – 2087.
[60] L. Xie, L. Jiao, H. Dai, *J. Am. Chem. Soc.* **2010**, *132*, 14751 – 14753.
[61] Z. Pan, N. Liu, L. Fu, Z. Liu, *J. Am. Chem. Soc.* **2011**, *133*, 17578 – 17581.
[62] D. V. Kosynkin, A. L. Higginbotham, A. Sinitskii, J. R. Lomeda, A. Dimiev, B. K. Price, J. M. Tour, *Nature* **2009**, *458*, 872 – 876.
[63] A. L. Higginbotham, D. V. Kosynkin, A. Sinitskii, Z. Sun, J. M. Tour, *ACS Nano* **2010**, *4*, 2059 – 2069.
[64] L. Jiao, L. Zhang, X. Wang, G. Diankov, H. Dai, *Nature* **2009**, *458*, 877 – 880.
[65] A. M. Affoune, B. L. V. Prasad, H. Sato, T. Enoki, Y. Kaburagi, Y. Hishiyama, *Chem. Phys. Lett.* **2001**, *348*, 17 – 20.
[66] L. G. Cançado, M. A. Pimenta, B. R. A. Neves, G. Medeiros-Ribeiro, T. Enoki, Y. Kobayashi, K. Takai, K.-i. Fukui, M. S. Dresselhaus, R. Saito, A. Jorio, *Phys. Rev. Lett.* **2004**, *93*, 047403.
[67] J. Lu, P. S. E. Yeo, C. K. Gan, P. Wu, K. P. Loh, *Nat. Nanotechnol.* **2011**, *6*, 247 – 252.
[68] K. P. Loh, Q. Bao, G. Eda, M. Chhowalla, *Nat. Chem.* **2010**, *2*, 1015 – 1024.
[69] a) W. Pisula, X. Feng, K. Müllen, *Adv. Mater.* **2010**, *22*, 3634 – 3649; b) W. Pisula, X. Feng, K. Müllen, *Chem. Mater.* **2011**, *23*, 554 – 567.
[70] C. D. Simpson, J. D. Brand, A. J. Berresheim, L. Przybilla, H. J. Räder, K. Müllen, *Chem. Eur. J.* **2002**, *8*, 1424 – 1429.
[71] a) J. Wu, W. Pisula, K. Müllen, *Chem. Rev.* **2007**, *107*, 718 – 747; b) W. Pisula, X. L. Feng, K. Müllen, *Chem. Mater.* **2011**, *23*, 554 – 567.
[72] X. L. Feng, W. Pisula, T. Kudernac, D. Q. Wu, L. J. Zhi, S. De Feyter, K. Müllen, *J. Am. Chem. Soc.* **2009**, *131*, 4439 – 4448.
[73] a) H. J. Räder, A. Rouhanipour, A. M. Talarico, V. Palermo, P. Samori, K. Müllen, *Nat. Mater.* **2006**, *5*, 276 – 280; b) A. Rouhanipour, M. Roy, X. Feng, H. J. Räder, K. Müllen, *Angew. Chem.* **2009**, *121*, 4672 – 4674; *Angew. Chem. Int. Ed.* **2009**, *48*, 4602 – 4604.
[74] a) E. Clar, *Ber. Dtsch. Chem. Ges.* **1929**, *62*, 1574 – 1582; b) E. Clar, C. T. Ironside, M. Zander, *J. Chem. Soc.* **1959**, 142 – 147; c) R. Scholl, C. Seer, *Justus Liebigs Ann. Chem.* **1912**, *394*, 111 – 177; d) R. Scholl, C. Seer, *Ber. Dtsch. Chem. Ges.* **1922**, *55*, 330 – 341; e) E. Clar, D. G. Stewart, *J. Am. Chem. Soc.* **1953**, *75*, 2667 – 2672.
[75] M. A. Ogliaruso, M. G. Romanelli, E. I. Becker, *Chem. Rev.* **1965**, *65*, 261 – 367.
[76] K. P. C. Vollhardt, *Angew. Chem.* **1984**, *96*, 525 – 541; *Angew. Chem. Int. Ed. Engl.* **1984**, *23*, 539 – 556.
[77] a) Z. Wang, Ž. Tomović, M. Kastler, R. Pretsch, F. Negri, V. Enkelmann, K. Müllen, *J. Am. Chem. Soc.* **2004**, *126*, 7794 – 7795; b) M. Kastler, J. Schmidt, W. Pisula, D. Sebastiani, K. Müllen, *J. Am. Chem. Soc.* **2006**, *128*, 9526 – 9534; c) X. Feng, W. Pisula, K. Müllen, *J. Am. Chem. Soc.* **2007**, *129*, 14116 – 14117.
[78] a) S. M. Draper, D. J. Gregg, R. Madathil, *J. Am. Chem. Soc.* **2002**, *124*, 3486 – 3487; b) M. Takase, V. Enkelmann, D. Sebastiani, M. Baumgarten, K. Müllen, *Angew. Chem.* **2007**, *119*, 5620 – 5623; *Angew. Chem. Int. Ed.* **2007**, *46*, 5524 – 5527.
[79] C. D. Simpson, G. Mattersteig, K. Martin, L. Gherghel, R. E. Bauer, H. J. Räder, K. Müllen, *J. Am. Chem. Soc.* **2004**, *126*, 3139 – 3147.
[80] J. Sakamoto, M. Rehahn, G. Wegner, A. D. Schlüter, *Macromol. Rapid Commun.* **2009**, *30*, 653 – 687.
[81] D. Wasserfallen, M. Kastler, W. Pisula, W. A. Hofer, Y. Fogel, Z. Wang, K. Müllen, *J. Am. Chem. Soc.* **2006**, *128*, 1334 – 1339.
[82] X. Zhang, X. Jiang, K. Zhang, L. Mao, J. Luo, C. Chi, H. S. O. Chan, J. Wu, *J. Org. Chem.* **2010**, *75*, 8069 – 8077.
[83] X. Feng, J. Wu, V. Enkelmann, K. Müllen, *Org. Lett.* **2006**, *8*, 1145 – 1148.
[84] X. Dou, X. Yang, G. J. Bodwell, M. Wagner, V. Enkelmann, K. Müllen, *Org. Lett.* **2007**, *9*, 2485 – 2488.
[85] A. Pradhan, P. Dechambenoit, H. Bock, F. Durola, *Angew. Chem.* **2011**, *123*, 12790 – 12793; *Angew. Chem. Int. Ed.* **2011**, *50*, 12582 – 12585.
[86] a) G. Beernink, M. Gunia, F. Dotz, H. Ostrom, K. Weiss, K. Müllen, C. Woll, *ChemPhysChem* **2001**, *2*, 317 – 320; b) K. Weiss, G. Beernink, F. Dotz, A. Birkner, K. Müllen, C. H. Woll, *Angew. Chem.* **1999**, *111*, 3974 – 3978; *Angew. Chem. Int. Ed.* **1999**, *38*, 3748 – 3752.
[87] X. Xue, L. T. Scott, *Org. Lett.* **2007**, *9*, 3937 – 3940.
[88] a) L. Grill, M. Dyer, L. Lafferentz, M. Persson, M. V. Peters, S. Hecht, *Nat. Nanotechnol.* **2007**, *2*, 687 – 691; b) J. A. Lipton-Duffin, O. Ivasenko, D. F. Perepichka, F. Rosei, *Small* **2009**, *5*, 592 – 597.
[89] U. Müller, M. Baumgarten, *J. Am. Chem. Soc.* **1995**, *117*, 5840 – 5850.
[90] J. Hassan, M. Sevignon, C. Gozzi, E. Schulz, M. Lemaire, *Chem. Rev.* **2002**, *102*, 1359 – 1469.
[91] M. Bieri, M.-T. Nguyen, O. Gröning, J. Cai, M. Treier, K. Aït-Mansour, P. Ruffieux, C. A. Pignedoli, D. Passerone, M. Kastler, K. Müllen, R. Fasel, *J. Am. Chem. Soc.* **2010**, *132*, 16669 – 16676.
[92] M. Bieri, S. Blankenburg, M. Kivala, C. A. Pignedoli, P. Ruffieux, K. Müllen, R. Fasel, *Chem. Commun.* **2011**, *47*, 10239 – 10241.
[93] Y. W. Son, M. L. Cohen, S. G. Louie, *Nature* **2006**, *444*, 347 – 349.